

Hybrid diamond/silicon suspended integrated photonic platform using SF₆ isotropic etching

Parashara Panduranga*, Aly Abdou*, Jens Richter†, Evan L H Thomas‡, Soumen Mandal‡
Zhong Ren§, Rasmus H Pedersen§, Oliver A Williams‡, Jeremy Witzens†, Maziar P Nezhad*¶

* School of Computer Science and Electronic Engineering, Bangor University, Bangor, UK

† Institute of Integrated Photonics, RWTH Aachen University, Aachen, Germany

‡ School of Physics and Astronomy, Cardiff University, Cardiff, UK

§ Oxford Instruments Plasma Technology, Bristol, UK

Email: ¶ maziar@bangor.ac.uk

Abstract—A hybrid diamond/silicon air-clad ridge waveguide platform is demonstrated. The air-clad structure coupled with the wide transmission window of diamond can allow for the use of this architecture over a large wavelength range, especially for the longer infrared wavelengths. In order to provide vertical confinement, the silicon substrate was isotropically etched using SF₆ plasma to create undercut diamond films. An in-depth analysis of the etch characteristics of this process was performed to highlight its potential to replace wet isotropic etching or XeF₂ isotropic vapour phase etching techniques. The performance of the waveguide at 1550 nm was measured, and yielded an average loss of 4.67 +/- 0.47 dB/mm.

Index Terms—diamond integrated photonics, infrared waveguides, isotropic etching, plasma etching, sulfur hexafluoride

I. INTRODUCTION

Group IV materials have become a reliable platform for integrated photonics, driven mainly by the suitability of silicon, silicon dioxide and silicon nitride as waveguide and cladding materials. However, the window of operational wavelengths of these materials is limited, hence necessitating the development of new materials and processes. Diamond is a wide band-gap semiconductor with a much larger optical transmission window compared to the aforementioned materials [1], and is therefore an excellent candidate for photonic chips operating in the UV, visible and infrared spectral regions. Several photonic components have been demonstrated using nanocrystalline diamond (NCD) grown refractive index substrates or buried layers to create vertical confinement [2]–[4]. Here we present air-clad suspended nanocrystalline diamond (NCD) waveguides fabricated using thin films directly grown on silicon substrates. This architecture not only creates the necessary vertical and lateral confinement needed to create a guided mode, it also offers a pathway for complete utilisation of the optical transmission window of diamond.

II. DESIGN

Since the NCD layer is grown on silicon substrates, the platform will not inherently possess vertical confinement, due

This work was supported by funding from the Welsh Government and Higher Education Funding Council for Wales through the Sêr Cymru National Research Network in Advanced Engineering and Materials (NRN 105) and also the UK Engineering and Physical Sciences Research Council (EPSRC) Innovation Fellowship grant EP/S001425/1.

to the considerably larger refractive index of silicon (3.47) compared to diamond (2.39). Therefore, we have created a suspended rib waveguide with air cladding above and below it, as shown in Figure 1. As a consequence, this design has advantage of being limited only by the diamond transmission window, and also offers a convenient platform for sensing applications, in particular gas sensing. Further details of the photonic design of this structure are available in [5].

The waveguide dimensions (waveguide width, etch depth and the bend radius) were calculated using a finite element solver (COMSOL). It was determined that a 350 nm etch depth along with a 600 nm waveguide width would ensure that the waveguide would support a single TE mode (Figure 2). An edge coupling setup was chosen to couple light in and out of the waveguides due to its broadband nature as well as its fabrication simplicity.

III. FABRICATION

A. NCD Growth

The NCD was grown on a 500 μm thick, highly doped silicon wafer, as reported in [6]. First, a mono-dispersed nanodiamond solution was applied in an ultra-sonic bath for 10 minutes to seed the silicon wafer. A 600 nm thick layer of diamond was grown on top of the silicon surface through

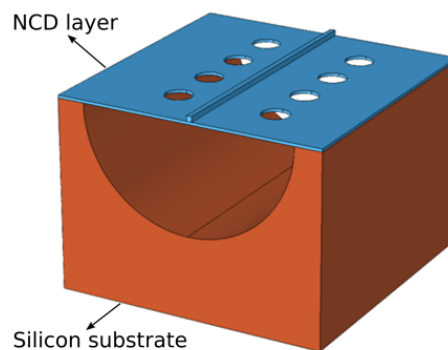


Fig. 1. Schematic of the suspended NCD waveguide.

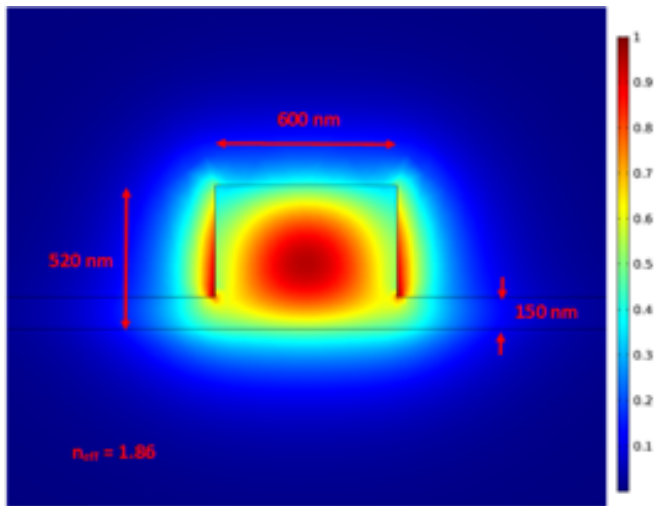


Fig. 2. The TE mode in the waveguide along with the designed waveguide dimensions.

CVD (CH_4 at 5 sccm; H_2 at 475 sccm; Pressure = 40 Torr; Power = 3500 W; Time: 298 minutes; Temperature = 842 °C). The film was grown with an initial 5 minute incubation period of 25 sccm CH_4 to establish the seeds before reducing to 5 sccm for the remainder of growth. The film was then thinned down to 520 nm through chemical mechanical polishing (using colloidal silica fluid, Logitech SF1) to achieve an RMS surface roughness value below 2 nm.

B. Fabrication

A series of waveguides ranging from 1.524 to 4.524 mm were chosen for this study, and were patterned through E-beam lithography using a hydrogen silsesquioxane (HSQ) mask. In order to form the ridge waveguide, the NCD layer was etched using RIE with O_2 at 30 sccm, pressure = 65 mTorr and RF power = 100 W. This recipe provided the desired vertical side walls and had an etch rate of about 60 nm/minute. Following this etch, the HSQ was removed using hydrofluoric acid (HF). Etch holes were patterned on the surface using optical lithography and a 40 nm chromium mask, and the diamond layer etched using the recipe mentioned above. This is depicted in Figure 3. These holes were 3.3 μm in diameter and were created in order to etch the underlying silicon layer isotropically. All wet processing steps were performed before undercutting the diamond film, to reduce the chances of damaging the undercut structures.

In order to form the suspended waveguide, isotropic etching of the underlying silicon substrate is necessary. Conventionally isotropic silicon etching has been performed through wet etching. This can often be problematic since the surface tension of the etchants can damage delicate structures and membranes. Alternatively, vapour phase etching (using etchants such as XeF_2) can also be used [7], [8]. Though this offers high selectivity to silicon with respect to aluminium, photoresist and silica, both the equipment required for the etch as well as the chemical itself are niche and somewhat expensive, making

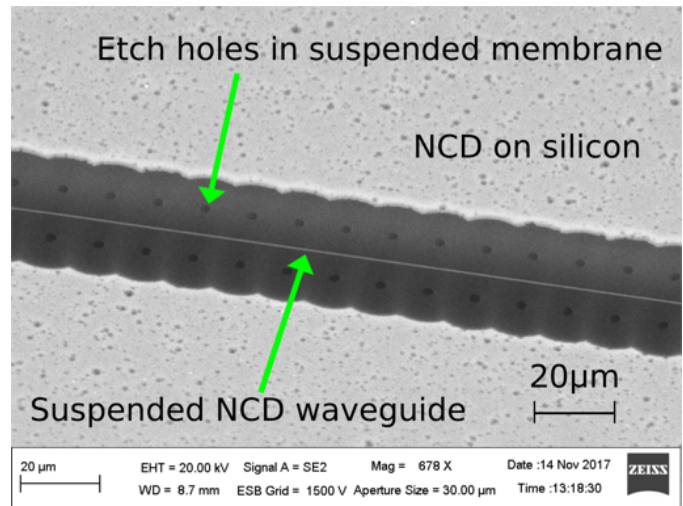


Fig. 3. SEM image of the undercut waveguide and membrane.

the process less economically viable. We have performed this etch using SF_6 plasma in an inductively coupled plasma (ICP)-RIE reactor (50 sccm SF_6 , 30 mTorr, 1500 W ICP power, 0 RF power). This etch rate of this process was constrained due to the holes affecting the neutral transport. This phenomenon also had the adverse side effect of causing the diamond membrane to sag at the edges, as the etch rate here was not constrained by the etch holes. This can be clearly seen in Figure 4. The behaviour of this process has not been well studied, and therefore we have studied the characteristics of this etch in depth.

C. SF_6 Etch Characteristics

It has been well established that silicon readily etches in fluorine-based gases and plasmas [9]. Though many fluorinated etchants are commercially used, SF_6 was chosen due

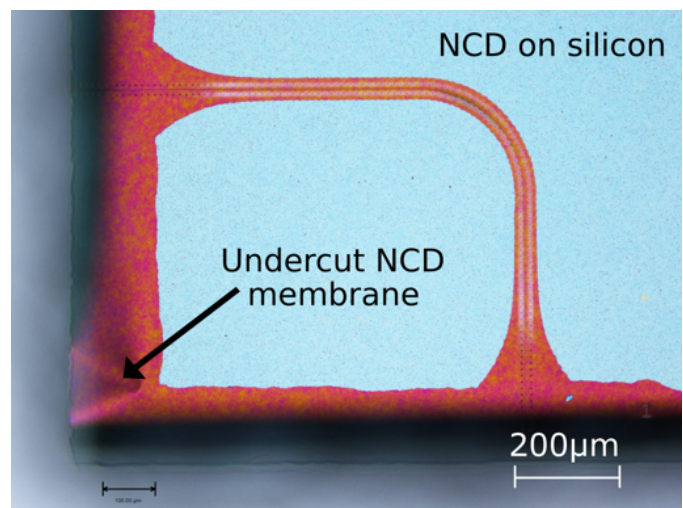


Fig. 4. Optical image of an undercut waveguide showing the sagging edges on the chip.

to the higher density of radicals, as well as its inert nature [10]. The degree of isotropy can be maximised by removing the physical component of the etch. This is achieved by only applying an inductively coupled excitation in an ICP-RIE etching chamber (i.e., setting the capacitive RF excitation to zero). The process parameters of importance for this application are the etch rate and surface roughness.

The samples for the study were prepared using thermally oxidised chips (approximately $1\text{ cm} \times 1\text{ cm}$ and oxide thickness of 290 nm) covered with a 100 nm thick layer of chromium. Optical lithography was used to pattern the samples with 8 circles of diameter $500\text{ }\mu\text{m}$ arranged diagonally across the chip with a $990\text{ }\mu\text{m}$ gap separating them. The pattern was transferred to the chromium layer using a commercially available etchant, and the oxide layer was etched using buffered oxide etch (BOE). This pattern was chosen in order to measure the etch rate of the process without the constraints of aspect ratio, micro-masking and other etching phenomena that are dependent on the features, sample size, etc., as the etch rate and roughness at the centre of the features can be approximately viewed as the etch rate of unpatterned silicon, due to the relatively large size of the circles. The etches were performed with and without the presence of a silicon wafer in order to measure the balance effect of the silicon wafer.

The etch rates of the samples etched with the presence of the silicon wafer were found to be range between $2.07\text{ }\mu\text{m}/\text{min}$ to $2.47\text{ }\mu\text{m}/\text{min}$ (Figure 5). This is similar to etch rates achieved through the conventional dry isotropic etching of silicon i.e, the vapour phase etching using XeF_2 (typically between $1\text{ }\mu\text{m}/\text{min}$ to $3\text{ }\mu\text{m}/\text{min}$) [11]. Figure 5 also presents the etch rate obtained without the balancing effect of the carrier wafer and shows that the etch rate without the presence of a silicon wafer is much higher as expected.

The surface roughness of the etch as well as the AFM

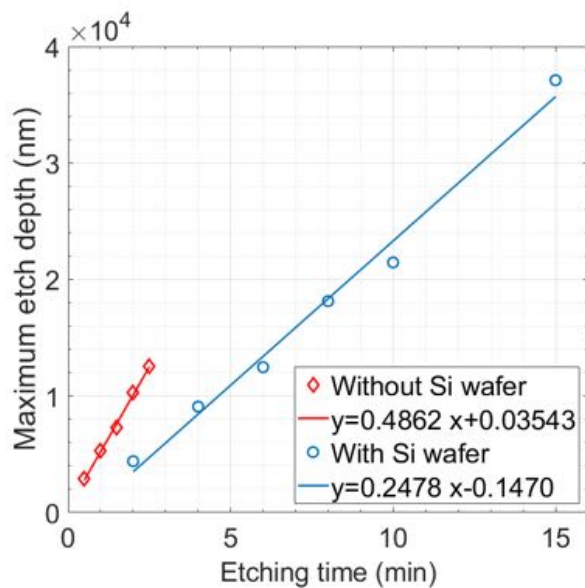


Fig. 5. Etch depth vs etch time with and without silicon carrier.

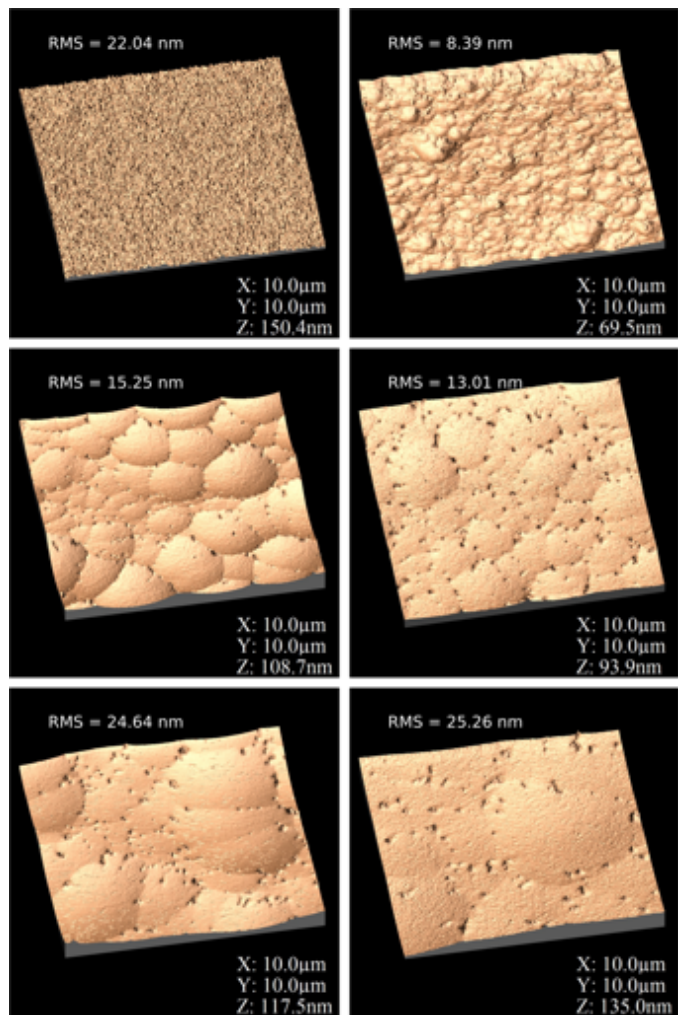


Fig. 6. AFM scans of the surface roughness for etch times of 2, 4, 6, 8, 10 and 15 minutes respectively. 'Z' is the maximum peak to valley measurement.

scans are presented in (Figure 6). It is evident that against the baseline roughness of the silicon ($< 1\text{ nm}$), the roughness initially rises. However, from the initial high, it slowly reduces with time, reaching its minimum value at 4 minutes, before increasing again. It can also be seen that the initial roughness is evenly spread features with small amplitude. As the etch time increases, areas of these features consolidate into larger and smoother "scallop" of larger amplitude. The roughness associated with this etch is expected, due to its chemical nature, and can be undesirable in an optical context, for example leading to scattering. A detailed study of this etching process has been presented in [12].

IV. OPTICAL MEASUREMENTS OF THE NCD WAVEGUIDE

Polarized light (at 1550 nm) from a tunable telecommunications laser was injected into the L-shaped waveguides using a lensed fiber. Due to the sag of the NCD membrane near the coupling region leading to non-constant coupling between waveguides, the scattered light approach was chosen to quantify the waveguide losses. The scattered light was

collected using a near-infrared camera viewing the chip from the top, as shown in (Figure 7). The obtained images were then processed to extract the optical losses by calculating the power drop along a horizontal or vertical segments of four different waveguides, under the assumption of uniform roughness scattering, and then fitting the results to an exponentially decaying function $P(L) = P(0)e^{-\alpha L}$ where $P(L)$ is the relative scattered power at the end of the segment and $P(0)$ is the relative power at the beginning of the segment. This yielded an average loss coefficient of 4.67 ± 0.47 dB/mm. Though these loss numbers are higher than reported values for single crystal diamond waveguides, they are in the vicinity or smaller than other reported NCD waveguides [4], [13], [14]. It is likely that most the losses are due to the surface roughness formed during the polishing step of the NCD deposition process. This is not an inherent issue with NCD films and can be addressed with appropriate adjustments to the growth and polishing steps.

V. CONCLUSION

We have demonstrated a hybrid silicon/diamond suspended air-clad waveguide platform fabricated from nanocrystalline diamond thin films utilising the SF₆ ICP etching process. We have also carried out an in-depth investigation of the SF₆ isotropic etch characteristics, and we have demonstrated its use as a viable alternative to other isotropic etch processes. This method presents an opportunity to perform these etches to isolate membranes, release MEMS structures etc., without the need for specialised etching equipment. The etch rates achieved during the study demonstrate that the etch duration can be comparable or faster than the XeF₂ vapour etch process. Though this structure was designed for operation at 1550 nm, this platform can be easily scaled to operate over a wide section of the optical spectrum, covering the UV to the far infrared and therefore can have a large range of applications ranging from visible light integrated photonics to far-infrared optical sensing.

VI. ACKNOWLEDGEMENT

We would like to acknowledge the cleanroom staff at Leeds University (LENNF), Manchester University (National Graphene Institute) and the University of California San Diego (NANO3) for their assistance with various aspects of fabricating the devices described here.

REFERENCES

- [1] Z. G. Hu, P. Prunici, P. Hess, and K. H. Chen, "Optical properties of nanocrystalline diamond films from mid-infrared to ultraviolet using reflectometry and ellipsometry," *Journal of Materials Science: Materials in Electronics*, vol. 18, no. S1, pp. 37–41, 2007.
- [2] V. Prajzler, M. Varga, P. Nektivindova, Z. Remes, and A. Kromka, "Design and investigation of properties of nanocrystalline diamond optical planar waveguides," vol. 21, no. 7, pp. 8417–8425, 2013.
- [3] N. Gruhler et al., "Diamond on aluminum nitride as a platform for integrated photonic circuits," vol. 213, no. 8, pp. 2075–2080, 2016.
- [4] P. Rath, N. Gruhler, S. Khasminskaya, C. Nebel, C. Wild, and W. Pernice, "Waferscale nanophotonic circuits made from diamond-on-insulator substrates," vol. 21, no. 9, pp. 11031–11036, 2013.
- [5] A. Abdou et al., "Air-clad suspended nanocrystalline diamond ridge waveguides," vol. 26, no. 11, pp. 13883–13890, 2018.

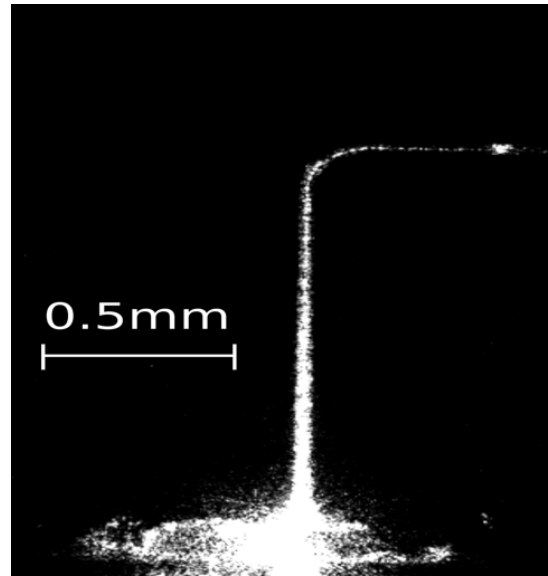


Fig. 7. IR image of the scattered light at 1.55 μm

- [6] E. L. Thomas, G. W. Nelson, S. Mandal, J. S. Foord, and O. A. Williams, "Chemical mechanical polishing of thin film diamond," vol. 68, pp. 473–479, 2014.
- [7] L. R. Arana, N. de Mas, R. Schmidt, A. J. Franz, M. A. Schmidt, and K. F. Jensen, "Isotropic etching of silicon in fluorine gas for MEMS micromachining," vol. 17, no. 2, p. 384, 2007.
- [8] P. B. Chu et al., "Controlled pulse-etching with xenon difluoride," presented at the Proceedings of international solid state sensors and actuators conference (Transducers' 97), 1997, vol. 1, pp. 665–668.
- [9] C. J. Mogab, "The loading effect in plasma etching," vol. 124, no. 8, pp. 1262–1268, 1977.
- [10] D. C. Hays et al., "Comparison of F 2-Based Gases for High-Rate Dry Etching of Si," vol. 146, no. 10, pp. 3812–3816, 1999.
- [11] D. Xu, B. Xiong, G. Wu, Y. Wang, X. Sun, and Y. Wang, "Isotropic Silicon Etching With XeF₂ Gas for Wafer-Level Micromachining Applications," vol. 21, no. 6, pp. 1436–1444, 2012.
- [12] P. Panduranga, A. Abdou, Z. Ren, R. H. Pedersen, and M. P. Nezhad, "Isotropic silicon etch characteristics in a purely inductively coupled SF₆ plasma," vol. 37, no. 6, p. 061206, 2019.
- [13] X. Checoury et al., "Nanocrystalline diamond photonics platform with high quality factor photonic crystal cavities," vol. 101, no. 17, p. 171115, 2012.
- [14] M. Malmström, M. Karlsson, P. Forsberg, Y. Cai, F. Nikolajeff, and F. Laurell, "Waveguides in polycrystalline diamond for mid-IR sensing," vol. 6, no. 4, pp. 1286–1295, 2016.